Journal of
Marine Science and Engineering

MDPI

Article

Uncertainty Assessment of the Remaining Volume of an Offshore Gravity Fish Cage

Zhongchi Liu and C. Guedes Soares *

Centre for Marine Technology and Ocean Engineering (CENTEC), Instituto Superior Técnico, Universidade de Lisboa, Av. Rovisco Pais, 1049-001 Lisboa, Portugal; zhongchi.liu@centec.tecnico.ulisboa.pt
* Correspondence: c.guedes.soares@centec.tecnico.ulisboa.pt

Abstract: The volume of a gravity cage is greatly reduced under a current due to the flexible structure, which affects the growth and health of the fish. Thus, an accurate assessment of cage volume is essential to determine the number of fishes in the cage. In this study, firstly, a numerical model was built to study the cage volume reduction of gravity cages due to the flexible net deformation when subjected to uniform flow. The remaining volume was calculated and compared with earlier experiments. Even though the flow velocity reductions were considered according to the data from previous experiments, the differences between the results from the numerical calculation and the towing tests are still significant. The physical model tests were treated as the reference value to investigate the uncertainty of the model results. Both the velocity-independent model error and velocity-dependent model error were calculated. With the help of the error models, the uncertainty of the remaining volume can be predicted. In addition, the velocity-dependent model error performs better in evaluating the uncertainty of the numerical calculation of the remaining culturing volume. Overall, the results show that the numerical model assisted by the model errors can calculate the cage volume accurately.

Keywords: offshore gravity fish cage; remaining volume; numerical model; model errors

check for updates

Citation: Liu, Z.; Guedes Soares, C. Uncertainty Assessment of the Remaining Volume of an Offshore Gravity Fish Cage. *J. Mar. Sci. Eng.* **2024**, *12*, 289. https://doi.org/10.3390/jmse12020289

Academic Editor: Abdellatif Ouahsine

Received: 23 December 2023
Revised: 23 January 2024
Accepted: 31 January 2024
Published: 5 February 2024

1. Introduction

As an essential source of fish for human beings, the product of aquaculture keeps increasing and has exceeded 50% of the total fish production [1]. The currents in offshore regions can provide abundant oxygen and a fresh environment which attracts people to establish fish farms there [2]. As a widely used fish cage, the gravity cage has a large culturing volume, which is, however, easily affected by currents and waves due to its flexible structure. The large deformation of the nets can reduce the culturing volume and threaten the fish's health and growth. Therefore, it is very important to develop an accurate method to predict the available cage volume, which is the major objective of this study.

Many studies have addressed the calculation of the structural responses of the cages subjected to current and waves. They focused on the loads on the cage, cage motions, net deformation, cage volumes, and other relative topics. Lader et al. [3] used pressure sensors to measure the cage volumes of full-scale rectangular and cylindrical gravity cages and provided information to determine the culturing fish number. Fu et al. [4] measured the hydrodynamic coefficients of a horizontal collar section using forced oscillation tests to achieve a high Keulegan–Carpenter number (KC). The results can help to improve the accuracy of the calculation when the Morison equation is applied.

Moe-Føre et al. [5] measured the hydrodynamic load and deformation of a small-scale cage in their experiment. They also built a numerical model to calculate the cage volume. It was found that the current calculation method is not accurate enough for cages with high-solidity nets. Gansel et al. [6] compared two methods to estimate the drag coefficients and the flow velocity reduction with their experimental results. They indicated that it is necessary to get a better understanding of the flow inside the cage. Huo et al. [7] calculated the mooring forces and assessed the fatigue damage under wave groups. The results can be used to evaluate the fatigue life of the mooring ropes. Liu et al. [8] described a numerical procedure to calculate the mooring forces and the cage motions for a gravity cage system.

Liu et al. [9] did experiments to study the wave attenuation induced by small-scale gravity cages in a flume. The results can be used to improve the accuracy of current calculation methods. They also measured the cage motion and the mooring forces in their experiments and the results can be used to verify the numerical calculations in further studies [10]. Cheng et al. [11] calculated the cage volumes and the mooring forces with different cage shapes and dimensions. They found that it is more effective to increase the width of the cage than the depth to protect the cage volume subjected to currents. Wang et al. [12] built a numerical model to study the motion and loads on a vessel-shaped cage array subjected to waves with different periods and heights. They compared the results with and without considering the diffraction and radiation waves. The results showed the necessity to account for the diffraction and radiation waves in the calculations. Ye et al. [13] provided a method for detecting wear in composite material ropes, which can be applied in the mooring system for gravity cage systems.

On the other hand, many researchers have also studied the flow field around the cages. Park et al. [14] used rotating vertical tubes to simulate a swimming fish school inside a cage and measured the fluid field. They found that the fish school can reduce both the drag force on the cage and the flow velocities. Wang et al. [15] found that the maximum velocities of water particles are increased by 39% and 21% in horizontal and vertical directions inside a vessel-shaped cage system. From their results, it is necessary to consider the diffraction and radiation waves when calculating the fluid field inside a cage. Yang et al. [16] built a CFD model to calculate the wake flow of a solid cage with a fixed bottom subjected to uniform flow. Their results can be used to check whether the water exchange is enough for the fish school inside the cage. Zeng et al. [17–19] compared flow field and mass-transport in the near-wake region of a rigid and of a flexible net panel for aquaculture in their experiments. They found that the rigid panel created a lower flow blockage and larger wake eddies, which contributed to generating favorable environments for fish growth.

For the present problem, different types and levels of uncertainty are also involved, including the 3-D downstream field, the coefficients of the Morison equation to calculate the net load, and other factors depending on the numerical models of fish cages, the setup of the experiment and the working environment. However, it is impossible to study each factor individually and find out their contribution to the final uncertainty. Thus, the model uncertainty is obtained by comparing the numerical model result with the experimental data from research [6], which is treated as the reference value.

As demonstrated in previous work [20], the current velocity has a great impact on the cage volume reduction. To compare with previous towing tests, the cage volume reduction subjected to uniform flow is calculated using the Finite Element Method (FEM) in the present work. Firstly, the cage volume is calculated without considering the flow reduction in the cage. In addition, a method used to estimate the drag force is used to apply the flow velocity reduction. The nets are divided into the upstream part and the downstream part. The velocity of the flow acting on the downstream part is attenuated to a certain extent relative to the flow velocity of the upstream area. However, the differences between the results from this method and the reference values from the experiments are still significant. In addition, it makes the deformation of the cage inconsistent with the actual situation.

Therefore, both a velocity-independent model error and velocity-dependent model error are calculated to study the effect of the velocity on the uncertainty. The model errors provide an overall assessment of the uncertainties in current calculations. The corrected numerical result by the model error is much closer to the result of the physical model, which is treated as the reference value. In addition, the uncertainty on the remaining culturing volume of the fish cage depends highly on the flow velocity. The finding in the present work shows the necessity to consider the uncertainty in the numerical model. The results can also contribute to the prediction of the cage volume reduction for full-scale cages. However, more data and accurate measurements are necessary to build a complete prediction system for the cage volume.

An introduction of the numerical model and its results are in Sections 2 and 3, respectively. The model uncertainty is assessed in Section 4. The limitation of the current experiment and numerical method is discussed in Section 5 and a summary is in Section 6.

2. Numerical Method

The implicit finite element method is used to calculate the cage volume subjected to uniform flow in Ansys/APDL. The flexible nets deform rapidly when subjected to uniform flow, which results in a volume reduction. The nets are modeled by continuous 3-D link elements with no bending stiffness. The solidity, as an important parameter of net structure, which is defined as the ratio between the projected area of the twines and the total area of a net mesh, is 0.27 in this work. The solidity is calculated by [21]:

$$S_n = \frac{2d}{L} - \left(\frac{d}{L}\right)^2$$

where S_n is the solidity of the net, d is the thickness of one twine and L is the width of one mesh.

To reduce the number of elements, dense twines are simplified into evenly distributed horizontal and vertical lines, as shown in Figure 1. The new structure has the same total cross-section area, tensional stiffness and mass as the original one. However, the new structure has a smaller projected area than the original structure. Thus, to get the same dynamic load, the drag coefficient is adjusted. The structural properties are listed in Table 1. More information on the FEM model can be found in research [20]. To calculate the volume fast and automatically, the coordinates of the nodes are recorded and input into a CAD software. The surrounded area forms a solid body, and then the volume is calculated.

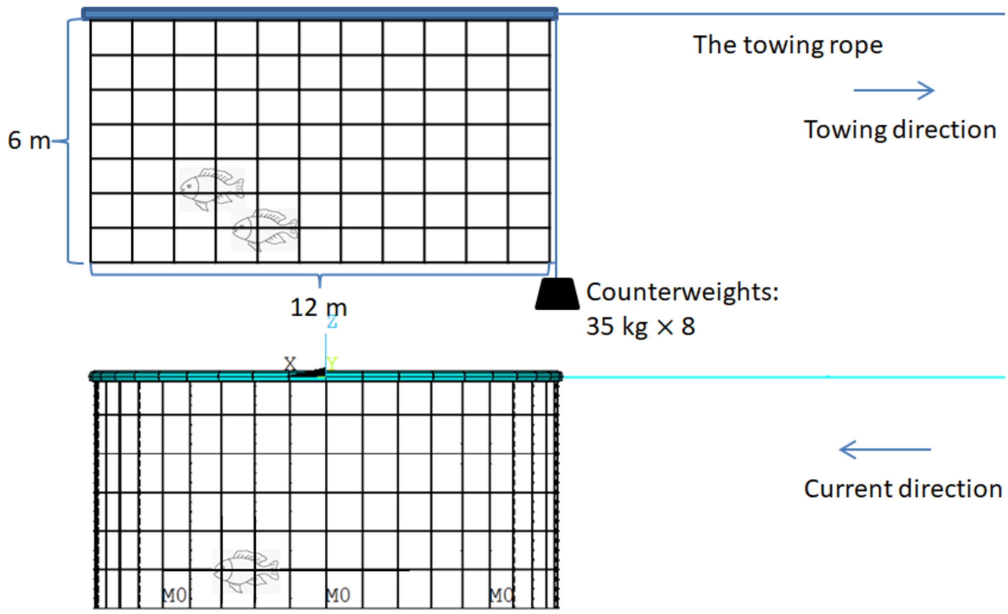

Figure 1. The schematic of the physical model from [6] (**upper**) and the numerical model (**lower**).

Table 1. Structural properties of the modeled net structure.

Properties	Adjusted Net Strucutres
Single twine diameter	2 mm
Number of horizontal lines	6
Number of vertical lines	40
Diameter of horizontal lines	17.07 mm
Diameter of vertical lines	16.57 mm
Young's modulus	3.5×10^6
Density	1015 kg/m^3
Mass of the counterweight	35 kg
Number of the counterweight	8

In addition, pipe elements are used to model the collar. The pipe element is a Timoshenko beam element with a hollow cross-section. The coupling of the bending and torsion is assumed to be negligible, which leads to the coincidence of the centroidal axis and the elastic axis. For a Timoshenko beam in the x-z plane, Hamilton's principle is expressed as:

$$\partial\Pi = \int_{t_1}^{t_2} (\delta U - \delta T - \delta W_e) dt = 0$$

where δU is the variation of the strain energy, δT is the variation of the kinetic energy, δW_e is the variation of the work from external forces.

The differential equations are expressed as [22,23]:

$$\frac{\partial}{\partial x}\left(\kappa G A\left(\frac{\partial w}{\partial x} + \theta\right)\right) + q = \rho A \frac{\partial^2 w}{\partial t^2}$$

$$\frac{\partial}{\partial x}\left(EI\frac{\partial \theta}{\partial x}\right) - \kappa G A\left(\frac{\partial w}{\partial x} + \theta\right) + m = \rho I \frac{\partial^2 \theta}{\partial t^2}$$

where w is the time-dependent transverse displacement of the centroidal axis, θ is the time-dependent rotation of the cross-section about the positive y-axis, κ is the Timoshenko shear coefficient, G is the shear modulus, A is the area of the cross-section, E is Young's modulus, I is the moment of inertia, ρ is the material density, q is the distributed force along the length of the beam and m is the distributed moments.

The counterweights are modeled by mass elements, which are added on eight notes according to the location of the physical model. The towing rope is modeled by a spring element. The height of the model is 6 m and the diameter of the model is 12 m. A total of 8 counterweights of 35 kg each are evenly distributed along the bottom circle of the model. To compare with the following result from the towing test [6], the numerical model is built as much as possible to be consistent with the physical model in the towing test, as shown in Figure 1. The flow direction is the positive x-axis direction. The dynamic equilibrium equation for the entire structure can be expressed as:

$$[M][\ddot{x}] + [C][\dot{x}] + [K][x] = G + f$$

where $[M]$, $[C]$ and $[K]$ are the mass, damping and stiffness matrix, respectively, $[\ddot{x}]$, $[\dot{x}]$ and $[x]$ are the acceleration, velocity and displacement vector, respectively, G is the gravity, f is the load on the structure including the buoyancy and the hydrodynamic load calculated from the Morison equation. A convergence analysis about the sizes of the elements can be found in the research [8].

In the experiment, pressure sensors were fixed on the net to measure the instantaneous position and the cage volume was calculated according to the measured results.

This test is chosen to compare with numerical results in this work due to the following reasons:

1. The test environment and experimental setup are close to the real working environment of a gravity cage under uniform flow.
2. The cage used in the test is full-scale for offshore aquaculture.
3. The authors provided enough information to build an approximate numerical model. The numerical model and the physical model are shown in Figure 1.

The process of measuring and calculating cage volumes in the experiment introduces uncertainties. For instance, the pressure sensors are only able to measure the vertical positions of the nets. They are supposed to move within planes parallel to the flow direction. The elongation of the nets is not taken into account, and the horizontal positions of the nets are determined based on the measured depths and the original net lengths. Furthermore, the entire cage volume is computed using data from only 16 sensors. The impact of these factors is uncertain and may result in errors. However, with current experimental capabilities, it is challenging to investigate these uncertainties in the experiments. Experimental results are the only and most convincing data that are directly from the measurement. Thus, the measured volumes in the experiment are treated as the reference values in this paper.

3. Numerical Results and Comparison with Test Results

3.1. Numerical Model without Considering Flow Velocity Reduction

In this section, the wake flow is not considered in the numerical model and the flow velocity is constant. The deformed cages subjected to different flow velocities are shown in Figure 2.

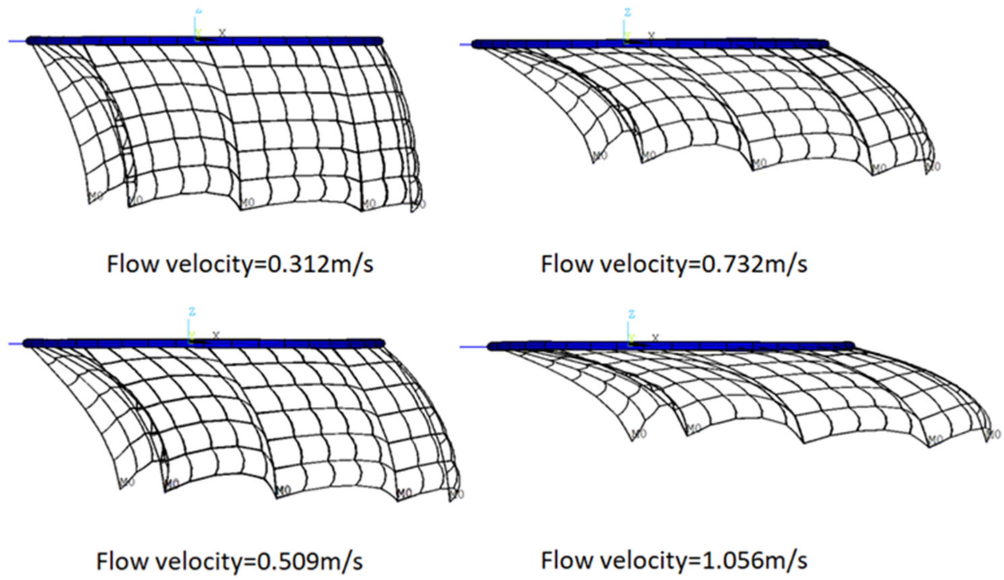

Figure 2. Deformation of the cage under different flow velocities.

The cages deformed more when they are subjected to more intense flow. The calculated remaining volumes (%) and the experiment results are listed in Table 2. The numerical model overestimates the cage's remaining volume, especially when subjected to large flow velocities. The difference between the two models subjected to a current of 0.312 m/s is only 5.3%, but it increases to 36.4% subjected to a current of 1.056 m/s.

Table 2. Remaining volume (%) of the cage from physical and numerical models.

Flow Velocity(m/s)	Volume of Physical Model	Volume of Numerical Model with no Flow Reduction	Volume of Numerical Model with Plan I Flow Reduction	Volume of Numerical Model with Plan II Flow Reduction
0.312	75%	79.2%	76.94%	77.44%
0.509	59%	70.17%	72.1%	68.57%
0.732	44%	59.45%	59.49%	55.89%
1.056	33%	45.02%	47.65%	47.2%

3.2. Numerical Model Subjected to Waves of Different Heights

To consider the wake flow in the numerical model, the structure is divided into two parts, the upstream part and the downstream part, as shown in Figure 3. The velocity of the flow acting on the downstream part is attenuated to a certain extent relative to the flow velocity of the upstream area. This method was used to calculate the drag forces and effectively reduced the difference between the experimental and numerical results.

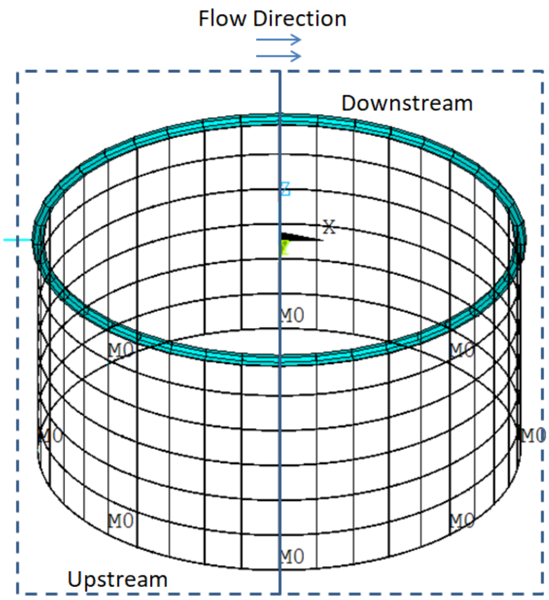

Figure 3. Upstream and downstream part of the cage.

Two plans of the velocity reduction ratio are applied in this work from Gansel et al. [24] and Zhao et al. [25], which are used to calculate the drag forces in research [6]. In Plan I, the velocity reduction ratio is set to 20% according to the cage dimension and its solidity. In addition, the reduction ratio of the flow velocity is assumed to depend highly on the upstream flow velocity in Plan II. The velocity reduction ratio is set to 50%, 70%, 70%, and 70%, respectively, at the flow velocity of 0.312 m/s, 0.509 m/s, 0.732 m/s and 1.056 m/s, as shown in Table 3.

Table 3. Velocity reduction ratio in the downstream area.

Flow Velocity (m/s)	Plan I	Plan II
0.312	20%	50%
0.509	20%	70%
0.732	20%	70%
1.056	20%	70%

The cage deformations with and without the flow reduction are compared in Figure 4. Because the upstream flow velocity is the same, the shapes of the upstream parts are almost the same. However, the horizontal displacement decreases with the downstream flow velocity for the downstream part. On the other hand, because of the reduction of the drag force and horizontal displacement, the depth of the cage in the downstream area increases with the reduction of the downstream flow velocity. Especially for the cages in the Plan II, the deformation of the downstream part is quite small compared with the ones from the cages of no flow velocity reduction and Plan I. This is mainly due to the large flow reduction ratios in the Plan II. For instance, when the upstream velocity is 0.732 m/s, the downstream flow velocity is only 0.22 m/s. Thus, the deformations of the downstream part in Plan II are much smaller than the ones from the rest two.

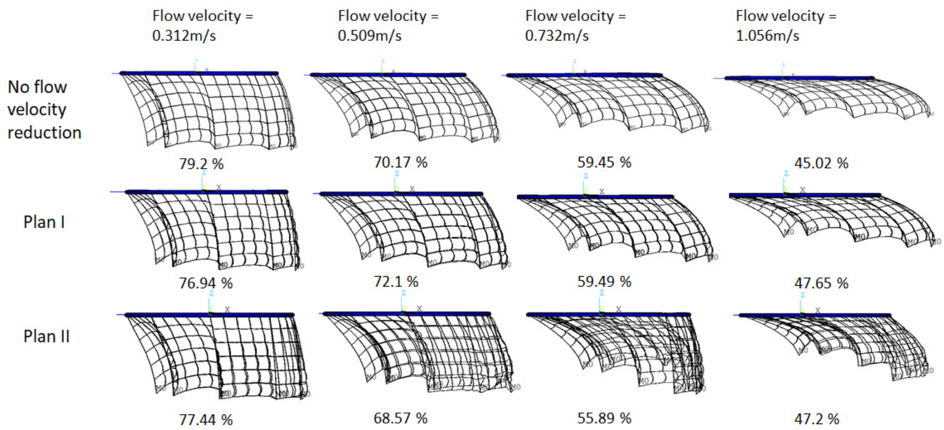

Figure 4. Deformation of the cage under uniform flow with and without considering the wake flow.

The remaining volumes of the cage are calculated and listed in Table 2. For Plan I, the volume only reduces the difference between the models at a flow velocity of 0.312 m/s. When the flow velocities are 0.509 m/s and 1.056 m/s, the differences are even larger than the ones with no flow reduction. For Plan II, it can reduce the differences at upstream flow velocities of 0.312 m/s. 0.509 m/s and 0.732 m/s. However, similarly to Plan I, when the upstream flow velocity is 1.056 m/s, the calculated volume is even larger than the numerical model with no flow reduction, which makes the difference larger. Additionally, for both plans, the reduction of the differences is insignificant. For instance, when the upstream flow velocity is 0.732 m/s, the smallest volume from the numerical models is 55.9%, which is 11.9% larger than the one from the physical model. Thus, this method of considering the flow reduction directly in the numerical model is not an effective one in the calculation of the cage remaining volume.

Furthermore, the upstream net has a much larger horizontal deformation than the downstream net, especially for Plan II. Around the border between the upstream and downstream net, the upstream part even moved to the right of the downstream part, which is never observed in experiments or field tests from [5,6,24–27]. It is due to the flow velocity downstream in Plan II being much smaller than the one upstream. The hydrodynamic load on the downstream part is much lower than the one acting on the upstream part. Additionally, when flow velocities are 0.732 m/s and 1.056 m/s for Plan II, the depths of the downstream net are much larger than the ones of the upstream net and the horizontal displacement is too small, which is also different from the observation of the experiment or field test.

Even though this method of considering wake flow effectively reduces the differences in drag forces, it failed to reduce the differences between the remaining volumes from the physical model and the numerical model. In addition, when the reduction of the wake flow velocity used in the numerical model is too large, the calculated cage shapes do not match the observed cage shapes under experiment and field tests. Thus, a better approach to calculating the cage volume is necessary.

4. Assessment of Model Uncertainty

Even though the flow reduction is considered in the last section, there are still differences between the numerical and physical models. Thus, a factor which represents the model uncertainty can be applied to adjust the calculated remaining volume from the numerical model and inform a better prediction of the cage volume subjected to uniform flow. The remaining volume can be influenced by many factors including the net solidity, the weight of the counterweight and flow velocity. In this work, except for the flow velocity, other factors are set to be constant to study how the remaining volume changes with the flow velocity. Thus, the model error is also assumed to be either velocity-independent or velocity-dependent. The wake flow is assumed to be included in the model uncertainty, so the numerical result used in this section is the one with no flow reduction.

4.1. Velocity-Independent Model Error

The model error is modeled here as velocity-independent and constant. Therefore, the relationship between the results from the models can be expressed as:

$$\widehat{V}_i = \phi V_i + \varepsilon_i, \phi = a, i = 1,2,3,4$$

where $\widehat{V}_i$ is the remaining volume from the physical model, V_i is the remaining volume from the numerical model and ε_i is the random error at a flow velocity v_i, ϕ is the model error function and it is a constant for velocity-independent model error.

The sum of squared errors can be expressed as:

$$Q = \sum (\varepsilon_i)^2 = \sum \left(\widehat{V}_i - aV_i\right)^2$$

The value of a with the smallest sum of squared errors can be expressed as:

$$a = \frac{\sum \widehat{x}_i x_i}{\sum x_i^2}$$

4.2. Velocity-Dependent Model Error

For the velocity-dependent model error, the relationship between the results from the models can be expressed as:

$$\widehat{V}_i = \phi(v_i) V_i + \varepsilon_i, \phi(v_i) = a + bv_i, i = 1,2,3,4$$

The sum of squared errors can be expressed as:

$$Q = \sum (\varepsilon_i)^2 = \sum \left(\widehat{V}_i - aV_i - bv_iV_i\right)^2$$

The values of a and b with the smallest sum of squared errors can be expressed as:

$$b = \frac{\sum \widehat{V}_i v_i V_i - \frac{\left(\sum \widehat{V}_i V_i\right)\left(\sum v_i V_i^2\right)}{\left(\sum V_i^2\right)}}{\sum v_i^2 V_i^2 - \frac{\left(\sum v_i V_i^2\right)^2}{\left(\sum V_i^2\right)}}$$

$$a = \frac{\sum \widehat{V}_i V_i - b \sum v_i V_i^2}{\sum V_i^2}$$

4.3. Results

Table 4 shows the calculated parameters in the velocity-independent model and velocity-dependent model. Table 5 shows the random errors and the squared errors Q of the two models. The adjusted remaining volumes from the two error models are closer to the physical results than the remaining volumes from numerical results.

Table 4. Calculated parameters in error models.

	Velocity-Independent Model	Velocity-Dependent Model
a	0.8592	1.0319
b	n/a.	−0.3333

Table 5. Random error ε_i and the sum of squared errors Q in the models.

Flow Velocity (m/s)	Velocity-Independent Model	Velocity-Dependent Model
0.312	0.0792	0.0169
0.509	−0.0044	−0.0136
0.732	−0.061	−0.0249
1.056	−0.0521	0.024
Q	0.0127	0.0017

The absolute value of the maximum random error from the velocity-dependent model is only 0.0249, while the one from the velocity-independent model is 0.0792, which is 2.18 times larger. The squared error from the velocity-dependent model is 0.0017, which is only 13.4% of that from the velocity-independent model. The remaining volumes of the physical, numerical and adjusted models are plotted in Figure 5. The plot of the velocity-dependent model is not only close to the physical results but also has the same trend. Thus, the velocity-dependent model is more adequate to characterize the effect of the uncertainty on the remaining culturing volume.

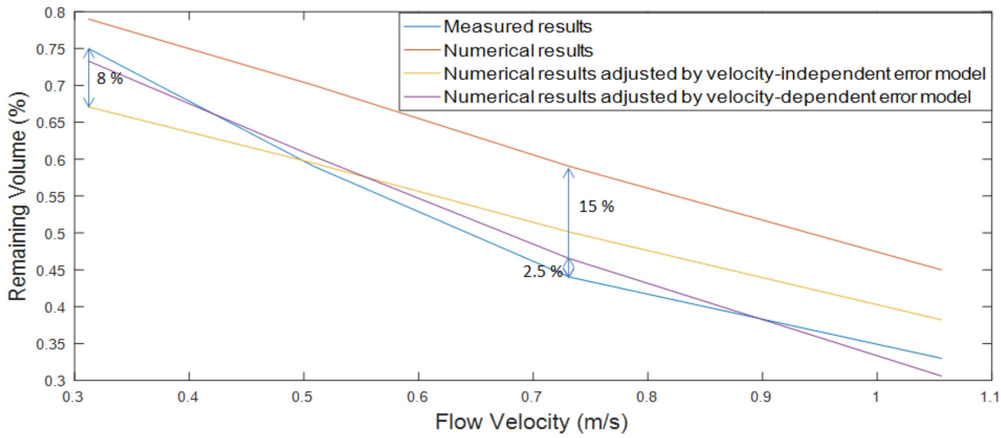

Figure 5. Remaining volumes of physical, numerical and adjusted models.

5. Discussion

In this section, firstly, the results of this work are compared with other published results to show the necessity of the model errors in the calculation. In addition, the current deficiencies and future research directions are discussed in Sections 5.2–5.4.

5.1. Comparison between the Results in This Work and Published Results

In addition to the comparison of the results in this paper, Dong et al. [28] listed the comparison of the remaining volume from other research. Zhao et al. [29] compared their numerical model with previous experimental results from Lader and Enerhaug [30]. The average difference between their numerical results and the experimental results is 4.3%. Lee et al. [31] also compared their calculation results with the experiment and the average difference is 5.9%. However, the difference increases when the reference values are from field tests rather than experiments. DeCew et al. [25] measured cage volumes with acoustic sensors near a harbor. The cage size is much larger than the ones in the lab and the average difference between their numerical and experimental results is 11.9%. Klebert et al. [27] measured the cage volumes of full-scale cages. The cage volume reduction of their experimental results is 1.3 times their numerical result on average. The differences are from the uncertainty of current technology, including the 3-D downstream field, the drag and inertia coefficients of the structure, and other factors depending on the numerical models of fish cages, the setup of the experiment and the operating environment.

On the other hand, the differences between the numerical and experimental results in this work are from 5.1% to 26.7%, and they increase with the current velocity. However, when the model errors are considered, the maximum difference reduces to 7.3% and the average value is 4.4%, even though the maximum current velocity in this work is 1.056 m/s, which is much larger than the current velocities in the experimental environment from the previous studies. From the numerical results of this and previous studies, it seems the numerical model alone cannot accurately estimate cage volume, especially under the real sea environment. Thus, the error models are applied to increase the accuracy of the numerical method. The small sums of squared errors in Section 4.3 and the comparison in this section show that the error models can assist the numerical model to improve the calculation accuracy.

Although the error model effectively compensates for the shortcomings of the numerical model, and assists in obtaining results closer to the reference values, the results obtained in this work cannot be directly applied to models with different characteristics. However, the method proposed in the paper can be applied to those other cases to determine how to improve their model predictions.

5.2. Increasing the Quantity of Experiment and Field Test Results

The results of the calculations in Section 4 shows that the approach presented in this paper is feasible for computing the volume of the gravity cage in the towing tests. As long as the parameters in the error model are calculated, it is possible to estimate the cage volume basing on the numerical results. The calculation method in this work can be developed into an alarm system when the upstream environment of the fish cage is monitored.

However, the flow velocity may not be the only factor that influences the model errors. More experiments and field tests are necessary to study other factors like cage dimensions, net solidities, counterweights, or any other factors that can influence the remaining volume of the cage. The error model is assumed to be a function of flow velocity. However, it can be a function of any other factor mentioned above. Currently, many experimental studies of cage motion and deformation are still in a laboratory environment. The experimental models are much smaller than offshore fish cages and many factors in the working environment are not included. Thus, to make a more complete uncertainty analysis, a large amount of experiments and field tests of full-scale fish cages in the working environment is necessary.

5.3. Improvement of the Experimental Technology

In addition to the quantity of experimental data, it is also necessary to find a better measurement method for cage volume. The locations of the nets are usually measured by pressure sensors. The dynamic pressure and the tension of the net are ignored. Furthermore, the number of sensors is also limited. Only 16 sensors are used in the towing test for a large fish cage of 12 m diameter and 6 m depth. The cage volumes are calculated from the shapes formed by the sensors. Thus, even though the experimental result is treated as the reference values in this work, it may not be accurate enough and further improvement or a new measurement method is necessary. In the further study, with more and better experimental results, it is possible to build empirical formula of the error models, which can be employed to assist numerical models for better calculating cage volumes.

5.4. Improvement of the Numerical Model

The calculated volume does not get close to the experimental result, no matter whether the wake flow is considered in the numerical model in this paper. The current method to consider the wake flow is to divide the net into two parts, the upstream part and the downstream part. However, the wake flow is three-dimensional and the effect of the net panels on the neighbors is ignored. If the wake flow can be a better description and applied to the numerical model, it will increase the calculation accuracy.

6. Conclusions

A numerical model of a gravity cage subjected to uniform flow is built to calculate the cage's remaining volume in this paper. The result is compared with a towing test of a fish cage with the same dimension, solidity and counterweight. To consider the flow velocity reduction, a method used in the drag force calculation is applied. The net structure is divided into the upstream and downstream parts, and the flow velocity applied on the downstream part is assumed to have a certain decrease relative to the velocity upstream. However, this method failed to reduce the differences between the numerical and physical models. In addition, if the velocity reduction value is too large in the numerical model, the cage deformation does not match the ones from the actual situation.

To make the prediction method more accurate, the numerical result is multiplied by a model error which presents the model uncertainty to adjust the result. Both velocity-independent and velocity-dependent models are calculated. Both models can improve the numerical result and make it closer to the experimental result, which is treated as the reference value in this paper. The velocity-dependent model has much smaller sums of squared errors, which shows that it is a better method to characterize the uncertainty. The sum of squared errors is only 0.0017 for the velocity-dependent model. It shows the model uncertainty of the remaining volume depends highly on the flow velocity. The limitation of this work and the further study directions are discussed. In order to facilitate broader application of the method in the paper, obtaining more accurate experimental results, particularly from experiments involving gravity cages of various dimensions, is essential. On the other hand, to obtain more accurate numerical results, precise descriptions of the flow field and accurate coefficients are also crucial.

Finally, it is important to note that the model uncertainty derived in this paper is associated with the calculation model and experimental results. The same model predictions compared with different experiments may lead to different values of the uncertainty, depending on the consistency of the different experimental results and different calculation models can have different model uncertainties with the same experimental results depending on the consistency of the calculation results.

Author Contributions: Conceptualization, C.G.S.; Methodology, Z.L.; Formal analysis, Z.L.; Writing—original draft, Z.L.; Writing—review & editing, C.G.S.; Visualization, Z.L.; Supervision, C.G.S. All authors have read and agreed to the published version of the manuscript.

Funding: The work was funded by the Portuguese Foundation for Science and Technology (Fundação para a Ciência e a Tecnologia-FCT), through a doctoral fellowship under Contract no. SFRH/BD/147178/2019. This work contributes to the Strategic Research Plan of the Centre for Marine Technology and Ocean Engineering (CENTEC), which is financed by the Portuguese Foundation for Science and Technology (Fundação para a Ciência e Tecnologia—FCT) under contract UIDB/UIDP/00134/2020.

Institutional Review Board Statement: Not applicable.

Informed Consent Statement: Not applicable.

Data Availability Statement: Data are contained within the article.

Conflicts of Interest: The authors declare no conflicts of interest.

References

1. FAO. *The State of World Fisheries and Aquaculture 2020*; Fisheries and Aquaculture Department, Food and Agriculture Organization of the United Nations: Rome, Italy; Publishing Policy and Support Branch, Office of Knowledge Exchange, Research and Extension: Rome, Italy, 2020.
2. Holmer, M. Environmental issues of fish farming in offshore waters: Perspectives, concerns and research needs. *Aquac. Environ. Interact.* **2010**, *1*, 57–70. [CrossRef]
3. Lader, P.; Dempster, T.; Fredheim, A.; Jensen, F. Current induced net deformations in full-scale cages for Atlantic salmon (*Salmo salar*). *Aquac. Eng.* **2008**, *38*, 52–65. [CrossRef]
4. Fu, S.; Xu, Y.; Hu, K.; Zhang, Y. Experimental investigation on hydrodynamics of floating cylinder in oscillatory and steady flows by forced oscillation test. *Mar. Struct.* **2013**, *34*, 41–55. [CrossRef]
5. Moe-Føre, H.; Lader, P.; Lien, E.; Hopperstad, O. Structural response of high solidity net cage models in uniform flow. *J. Fluids Struct.* **2016**, *65*, 180–195. [CrossRef]
6. Gansel, L.; Oppedal, F.; Birkevold, J.; Tuene, S. Drag forces and deformation of aquaculture cages-Full-scale towing tests in the field. *Aquac. Eng.* **2018**, *81*, 46–56. [CrossRef]
7. Hou, H.; Dong, G.; Xu, T. Assessment of fatigue damage of mooring line for fish cage under wave groups. *Ocean. Eng.* **2020**, *210*, 107568. [CrossRef]
8. Liu, Z.; Mohapatra, S.; Guedes Soares, C. Finite Element Analysis of the Effect of Currents on the Dynamics of a Moored Flexible Cylindrical Net Cage. *J. Mar. Sci. Eng.* **2021**, *9*, 159. [CrossRef]
9. Liu, Z.; Guedes Soares, C. Experimental Study of the Behaviour of a Circular Gravity Cage in Linear Waves. *Aquac. Eng.* **2022**, *99*, 102291. [CrossRef]
10. Liu, Z.; Xu, H.; Guedes Soares, C. Experimental study on the mooring forces and motions of a fish cage under regular waves. *Ocean Eng.* **2023**, *280*, 114612. [CrossRef]
11. Cheng, H.; Li, L.; Ong, M. Comparative study of five commonly used gravity type fish cages under pure current conditions. *Ocean Eng.* **2022**, *250*, 110977. [CrossRef]
12. Wang, Y.; Fu, S.; Xu, Y.; Li, S.; Moan, T. Loads on a vessel-shaped fish cage steel structures, nets and connectors considering the effects of diffraction and radiation waves. *Mar. Struct.* **2022**, *86*, 103301. [CrossRef]
13. Ye, H.; Li, W.; Lin, S.; Ge, Y.; Lv, Q. A framework for fault detection method selection of oceanographic multi-layer winch fibre rope arrangement. *Measurement* **2024**, *2024*, 114168. [CrossRef]
14. Park, S.; Zhou, J.; Dong, S.; Li, Q.; Yoshida, T.; Kitazawa, D. Characteristics of the flow field inside and around a square fish cage considering the circular swimming pattern of a farmed fish school: Laboratory experiments and field observations. *Ocean Eng.* **2022**, *261*, 112097. [CrossRef]
15. Wang, G.; Martin, T.; Huang, L.; Bihs, H. Numerical investigation of the hydrodynamics of a submersible steel-frame offshore fish farm in regular waves using CFD. *Ocean Eng.* **2022**, *256*, 111528. [CrossRef]
16. Yang, C.; Yuan, H.; Bai, X.; Hao, Z.; Sun, Y.; Wu, D.; Johanning, L. Numerical investigations on fluid characteristics around the bottom-fixed aquacultural farm. *Ocean Eng.* **2022**, *266*, 112689. [CrossRef]
17. Zeng, X.; Gualtieri, C.; Cuthbertson, A.; Shao, D. Experimental study of flow and mass transport in the near-wake region of a rigid planar metal net panel. *Aquac. Eng.* **2022**, *98*, 102267. [CrossRef]
18. Shao, D.; Huang, L.; Wang, R.-Q.; Gualtieri, C.; Cuthbertson, A. Flow turbulence characteristics and mass transport in the near-wake region of an aquaculture cage net panel. *Water* **2021**, *13*, 294. [CrossRef]
19. Yang, X.; Zeng, X.; Gualtieri, C.; Cuthbertson, A.; Wang, R.-Q.; Shao, D. Numerical Simulation of Scalar Mixing and Transport through a Fishing Net Panel. *J. Mar. Sci. Eng.* **2022**, *10*, 1511. [CrossRef]
20. Liu, Z.; Guedes Soares, C. Sensitivity analysis of a numerical model of the dynamics of gravity cages subjected to current and waves. *Ocean Eng.* **2023**, *287*, 115715. [CrossRef]
21. Fredheim, A. Current Forces on Net Structures. Ph.D. Thesis, NTNU Trondheim, Trondheim, Norway, 2005.
22. Friedman, Z.; Kosmatka, J. An improved two-node Timoshenko beam finite element. *Comput. Struct.* **1993**, *47*, 473–481. [CrossRef]
23. Kosmatka, J. An improved two-node finite element for stability and natural frequencies of axial-loaded Timoshenko beams. *Comput. Struct.* **1995**, *57*, 141–149. [CrossRef]
24. Gansel, L.C.; McClimans, T.A.; Myrhaug, D. Average flow inside and around fish cages with and without fouling in a uniform flow. *J. Offshore Mech. Arct. Eng. Trans. ASME* **2012**, *134*, 041201. [CrossRef]
25. Zhao, Y.-P.; Bi, C.-W.; Chen, C.-P.; Li, Y.-C.; Dong, G.-H. Experimental study on flow velocity and mooring loads for multiple net cages in steady current. *Aquac. Eng.* **2015**, *67*, 24–31. [CrossRef]
26. DeCew, J.; Fredriksson, D.W.; Lader, P.F.; Chambers, M.; Howell, W.H.; Osienki, M.; Celikkol, B.; Frank, K.; Høy, E. Field measurements of cage deformation using acoustic sensors. *Aquac. Eng.* **2013**, *57*, 114–125. [CrossRef]
27. Klebert, P.; Patursson, Ø.; Endresen, P.; Rundtop, P.; Birkevold, J.; Rasmussen, H. Three-dimensional deformation of a large circular flexible sea cage in high currents: Field experiment and modeling. *Ocean Eng.* **2015**, *104*, 511–520. [CrossRef]
28. Dong, G.; Hou, H.; Xu, T. Model uncertainty in hydrodynamic characteristics by numerical models for aquaculture plant and mooring system. *Ocean Eng.* **2021**, *219*, 108383. [CrossRef]
29. Zhao, Y.P.; Li, Y.C.; Dong, G.H.; Gui, F.K.; Teng, B. Numerical simulation of the effects of structure size ratio and mesh type on three-dimensional deformation of the fishing-net gravity cage in current. *Aquac. Eng.* **2007**, *36*, 285–301. [CrossRef]

30. Lader, P.F.; Enerhaug, B. Experimental investigation of forces and geometry of a net cage in uniform flow. *IEEE J. Ocean. Eng.* **2005**, *30*, 79–84. [CrossRef]
31. Lee, C.W.; Kim, Y.B.; Lee, G.H.; Choe, M.Y.; Lee, M.K.; Koo, K.Y. Dynamic simulation of a fish cage system subjected to currents and waves. *Ocean Eng.* **2008**, *35*, 1521–1532. [CrossRef]